

# p-wave and d-wave superconductivity in quasi-2D metals

P. Monthoux and G.G. Lonzarich

*Cavendish Laboratory, University of Cambridge*

*Madingley Road, Cambridge CB3 0HE*

(September 22, 2018)

## Abstract

We compare predictions of the mean-field theory of superconductivity for nearly antiferromagnetic and nearly ferromagnetic metals in two dimensions. The calculations are based on a parametrization of the effective interaction arising from the exchange of magnetic fluctuations. The Eliashberg equations for the transition temperature are solved including the full momentum dependence of the electron self-energy. The results show that for comparable parameters d-wave singlet pairing in nearly antiferromagnetic metals is generally much stronger than p-wave triplet pairing in nearly ferromagnetic metals in quasi two dimensions. The relevance to the layered materials, and in particular  $Sr_2RuO_4$  that exhibits p-wave triplet pairing, is discussed.

PACS Nos. 74.20.Mn

## I. INTRODUCTION

There is growing experimental evidence of anisotropic forms of superconductivity in the quasi two-dimensional perovskite oxides. Energy gaps of d-wave character have been established for some of the copper oxides that have strongly enhanced antiferromagnetic susceptibilities and high superconducting transition temperatures (of the order of  $100^\circ K$ )<sup>1-5</sup>. On the other hand, p-wave spin-triplet pairing provides a better understanding of the experimental data in the ruthenate  $Sr_2RuO_4$  that appears to be close to ordering ferromagnetically and becomes superconducting only at low temperature (of the order of  $1^\circ K$ )<sup>25,17,29,24,12-16</sup>.

Numerous mechanisms have been proposed for anisotropic superconductivity, especially in the cuprates. One of the most extensively investigated theoretically is based on a magnetic interaction arising via the exchange of enhanced antiferromagnetic spin-fluctuations<sup>6-10</sup>. Though not entirely without difficulties, this mechanism correctly anticipated from the beginning the d-wave symmetry of the order parameter observed in some of the copper oxides. Moreover, when treated in the mean-field Eliashberg theory with full momentum dependence of the electron self-energy, it provided an account of the high transition temperatures in the cuprates, in terms of parameters determined independently from normal state properties alone.

In this paper we include the case where, in contrast to the cuprates, a magnetic interaction between electron quasiparticles arises from the exchange of ferromagnetic instead of antiferromagnetic spin-fluctuations in quasi two-dimensional (2D) compounds. Our calculations differ from those previously reported<sup>19,20</sup> for p-wave triplet pairing in the following ways: (i) they concern quasi 2D rather than 3D systems, (ii) employ a non-parabolic band structure which has potential relevance to real compounds, and (iii) make use of the full Green's function in place of a simple pole approximation for the propagator. The latter (iii) takes a better account of the momentum dependence of the electron self-energy and was found to be important in the nearly antiferromagnetic 2D systems<sup>10</sup>. Comparisons of the mean-field Eliashberg equations for nearly ferromagnetic and nearly antiferromagnetic

metals with a single 2D Fermi surface are presented for a range of parameters defining the magnetic interaction in potentially realistic cases. The results show that the incipient ferromagnets are expected to have p-wave (spin-triplet) pairing and transition temperatures that are much lower than in the nearly antiferromagnetic metals for otherwise similar conditions. A physical interpretation of the numerical analyses is given together with a discussion of the possible relevance of the magnetic interaction model for  $Sr_2RuO_4$ . The mean-field analysis is intended as a first step toward a more complete treatment of superconductivity in highly correlated electron systems. It may also serve as a possible guide to future experiments to test for the existence of magnetically mediated superconductivity in general.

The outline of the paper goes as follows. In the next section we describe the model and computational method used in this work. In section III, we describe the results of the numerical calculations for both ferromagnetically and antiferromagnetically correlated metals. Section IV contains further discussion while our conclusions are presented in the final section.

## II. MODEL

We consider quasiparticles on a two-dimensional square lattice. We assume that the dominant scattering mechanism is of magnetic origin and postulate the following low-energy effective action for the quasiparticles:

$$S_{eff} = \sum_{\mathbf{p}, \alpha} \int_0^\beta d\tau \psi_{\mathbf{p}, \alpha}^\dagger(\tau) (\partial_\tau + \epsilon_{\mathbf{p}} - \mu) \psi_{\mathbf{p}, \alpha}(\tau) - \frac{g^2}{6} \sum_{\mathbf{q}} \int_0^\beta d\tau \int_0^\beta d\tau' \chi(\mathbf{q}, \tau - \tau') \mathbf{s}(\mathbf{q}, \tau) \cdot \mathbf{s}(-\mathbf{q}, \tau') \quad (1)$$

The spin density  $\mathbf{s}(\mathbf{q}, \tau)$  is given by

$$\mathbf{s}(\mathbf{q}, \tau) \equiv \sum_{\mathbf{p}, \alpha, \gamma} \psi_{\mathbf{p}+\mathbf{q}, \alpha}^\dagger(\tau) \sigma_{\alpha, \gamma} \psi_{\mathbf{p}, \gamma}(\tau) \quad (2)$$

where  $\sigma$  denotes the three Pauli matrices. The quasiparticle dispersion relation is

$$\epsilon_{\mathbf{p}} = -2t(\cos(p_x a) + \cos(p_y a)) - 4t' \cos(p_x a) \cos(p_y a) \quad (3)$$

with hopping matrix elements  $t$  and  $t'$ .  $\mu$  denotes the chemical potential,  $\beta$  the inverse temperature,  $g^2$  the coupling constant and  $\psi_{\mathbf{p},\sigma}^\dagger$  and  $\psi_{\mathbf{p},\sigma}$  are Grassmann variables. In the following we shall measure temperatures, frequencies and energies in the same units. Having in mind a possible connection to  $Sr_2RuO_4$ , we shall model the sheet of the Fermi surface of that material thought to be the most relevant for superconductivity<sup>25,28</sup> by choosing  $t'=0.45t$ . With an average Fermi wavevector of  $k_F \approx 0.7\text{\AA}^{-1}$  and a lattice constant  $a = 3.86\text{\AA}$ , Luttinger's theorem gives a doping  $n \approx 1.1$ . In the following, we shall adopt the value  $n = 1.1$ . The Fermi surface is shown in fig.(1).

Previous studies of the dependence of the critical temperature on the ratio  $t'/t$  and doping level<sup>26,27</sup> have shown the relative insensitivity of  $T_c$  to small changes in these parameters. Therefore, a more realistic description of the Fermi surface sheet of  $Sr_2RuO_4$  is not expected to alter our conclusions. We also note that deviations from the assumed 2D form of the Fermi surface sheet is found experimentally to be small.

Our model assumes that the coupling parameter  $g$  is constant. The  $\mathbf{q}$  dependence in the simplest case arises from the atomic form factor. For tight binding bands the latter is local in space and this leads to a weak dependence of  $g$  on  $\mathbf{q}$ . Moreover, near a magnetic instability the dominant  $\mathbf{q}$  dependence of the interaction is expected to arise from  $\chi(\mathbf{q}, \omega)$ , rather than that of  $g$ .

The retarded generalized magnetic susceptibility  $\chi(\mathbf{q}, \omega)$  that defines the effective interaction, Eq. (1), is assumed to take the phenomenological form

$$\chi(\mathbf{q}, \omega) = \frac{\chi_0 \kappa_0^2}{\kappa^2 + \hat{q}^2 - i \frac{\omega}{\eta(\hat{q})}} \quad (4)$$

$\kappa$  and  $\kappa_0$  are the inverse correlation lengths (in units of  $a^{-1}$ ) with and without of strong magnetic correlations respectively. Let

$$\hat{q}_\pm^2 = 4 \pm 2(\cos(q_x a) + \cos(q_y a)) \quad (5)$$

In the case of ferromagnetic correlations, the parameters  $\hat{q}^2$  and  $\eta(\hat{q})$  are defined as

$$\hat{q}^2 = \hat{q}_-^2 \quad (6)$$

$$\eta(\hat{q}) = T_{sf}\hat{q}_- \quad (7)$$

where  $T_{sf}$  is a characteristic spin-fluctuation temperature. We shall also investigate antiferromagnetic correlations, in which case these parameters take the form

$$\hat{q}^2 = \hat{q}_+^2 \quad (8)$$

$$\eta(\hat{q}) = T_{sf}\hat{q}_- \quad (9)$$

The spin-fluctuation propagator on the imaginary axis,  $\chi(\mathbf{q}, i\nu_n)$  is related to the imaginary part of the response function  $Im\chi(\mathbf{q}, \omega)$ , Eq. (4), via the spectral representation

$$\chi(\mathbf{q}, i\nu_n) = - \int_{-\infty}^{+\infty} \frac{d\omega}{\pi} \frac{Im\chi(\mathbf{q}, \omega)}{i\nu_n - \omega} \quad (10)$$

To get  $\chi(\mathbf{q}, i\nu_n)$  to decay as  $1/\nu_n^2$  as  $\nu_n \rightarrow \infty$ , as it should, we introduce a cutoff  $\omega_0$  and take  $Im\chi(\mathbf{q}, \omega) = 0$  for  $\omega \geq \omega_0$ . A natural choice for the cutoff is  $\omega_0 = \eta(\hat{q})\kappa_0^2$ . We have checked that our results for the critical temperature are not sensitive to the particular choice of  $\omega_0$  used.

The two-dimensional Eliashberg equations for the critical temperature  $T_c$  in the Matsubara representation reduce, for the effective action Eq. (1), to

$$\Sigma(\mathbf{p}, i\omega_n) = g^2 \frac{T}{N} \sum_{\Omega_n} \sum_{\mathbf{k}} \chi(\mathbf{p} - \mathbf{k}, i\omega_n - i\Omega_n) G(\mathbf{k}, i\Omega_n) \quad (11)$$

$$G(\mathbf{p}, i\omega_n) = \frac{1}{i\omega_n - (\epsilon_{\mathbf{p}} - \mu) - \Sigma(\mathbf{p}, i\omega_n)} \quad (12)$$

$$\begin{aligned} \lambda(T)\Phi(\mathbf{p}, i\omega_n) &= \left[ \frac{g^2}{3} \right] \frac{T}{N} \sum_{\Omega_n} \sum_{\mathbf{k}} \chi(\mathbf{p} - \mathbf{k}, i\omega_n - i\Omega_n) |G(\mathbf{k}, i\Omega_n)|^2 \Phi(\mathbf{k}, i\Omega_n) \\ \lambda(T) = 1 &\longrightarrow T = T_c \end{aligned} \quad (13)$$

where  $\Sigma(\mathbf{p}, i\omega_n)$  is the quasiparticle self-energy,  $G(\mathbf{p}, i\omega_n)$  the one-particle Green's function and  $\Phi(\mathbf{p}, i\omega_n)$  the anomalous self-energy.  $\epsilon_{\mathbf{p}}$  is the bare quasiparticle spectrum, Eq. (3),  $\mu$  the chemical potential that is adjusted to give an electron density of  $n = 1.1$ , and  $N$  the total number of allowed wavevectors in the Brillouin Zone. In Eq. (13), the prefactor  $g^2/3$

is for triplet pairing while the prefactor  $-g^2$  is appropriate for singlet pairing. Only the longitudinal spin-fluctuation mode contributes to the pairing amplitude in the triplet channel and gives rise to an attractive interaction. Both transverse and longitudinal spin-fluctuation modes contribute to the pairing amplitude in the singlet channel and give an interaction which is repulsive in reciprocal space with a peak at  $\mathbf{Q} = (\pi/a, \pi/a)$ . When Fourier transformed, such a potential is repulsive on one sublattice (even sites) and attractive on the other (odd sites). All three modes contribute to the quasiparticle self-energy.

The momentum convolutions in Eqs. (11,13) are carried out with a Fast Fourier Transform algorithm on a  $128 \times 128$  lattice. The frequency sums in both the self-energy and linearized gap equations are treated with the renormalization group technique of Pao and Bickers<sup>11</sup>. We have kept between 8 and 16 Matsubara frequencies at each stage of the renormalization procedure, starting with an initial temperature  $T_0 = 0.4t$  and cutoff  $\Omega_c \approx 20t$ . The renormalization group acceleration technique restricts one to a discrete set of temperatures  $T_0 > T_1 > T_2 \dots$ . The critical temperature at which  $\lambda(T) = 1$  in Eq. (13) is determined by linear interpolation. The savings in computer time and memory requirements afforded by this technique allowed us to study a wide range of temperatures and spin-fluctuation spectrum parameters.

### III. RESULTS

The dimensionless parameters at our disposal are  $g^2\chi_0/t$ ,  $T_{sf}/t$ ,  $\kappa_0$  and  $\kappa$ . It is found experimentally that  $T_{sf}\kappa_0^2 \approx \text{const}$ , and we shall use this relation to eliminate one parameter from the set and pick a representative value of the product  $T_{sf}\kappa_0^2$ . A value of  $T_{sf} = \frac{2}{3}t$  corresponds to about  $1000^\circ K$  for a bandwidth of 1 eV while a value of  $\kappa_0^2 \approx 12$  is representative of what one obtains from a Lindhard function with 2D parabolic bands for a Fermi momentum of about  $0.7\text{\AA}^{-1}$ .

The parameters of the model can in principle be inferred from the electronic structure, the dynamical magnetic susceptibility, and the resistivity in the normal state. The resistivity

in particular may be used to estimate the dimensionless coupling parameter  $g^2\chi_0/t$ , the value of which is between 10 and 20 for the simplest RPA approximation for the magnetic interaction potential.

The results of our numerical calculations of the mean-field critical temperature  $T_c$  in the case of a nearly ferromagnetic metal are shown in figs.(2),(3) and (4) for various values of the characteristic spin-fluctuation temperature  $T_{sf}$ . We find an instability for a p-wave gap function  $\Phi(\mathbf{p}, i\omega_n)$  transforming as  $\sin(p_x a)$  (or  $\sin(p_y a)$ , the two being degenerate for a square lattice).

Figs.(2a),(3a) and (4a) show  $T_c$  versus the dimensionless coupling parameter  $g^2\chi_0/t$  for several values of the square of the inverse correlation length parameter  $\kappa^2$  while figs.(2b), (3b) and (4b) show  $T_c$  versus  $\kappa^2$  for several values of the coupling parameter  $g^2\chi_0/t$ . The parameter  $\kappa^2$  can be varied experimentally by applying pressure to the samples. The  $T_c$  versus  $\kappa^2$  graphs can be interpreted as  $T_c$  versus pressure plots, with the critical pressure corresponding to the quantum critical point at  $\kappa^2 = 0$ . The critical temperature saturates, in the strong coupling limit, to a value of about  $T_{sf}/30$  for values of  $\kappa^2$  of 0.5 to 1.0. For long correlation lengths,  $T_c$  decreases. For fixed coupling constant  $g^2\chi_0/t$ , we find that the Eliashberg renormalization factor  $Z(\mathbf{p}, i\omega_n) = 1 - \text{Im}\Sigma(\mathbf{p}, i\omega_n)/\omega_n$  increases as  $\kappa^2$  decreases and thus pair-breaking effects tend to cancel the stronger attraction as  $\kappa \rightarrow 0$ , leading to the reduction of the transition temperature. For short correlation lengths,  $T_c$  is reduced as well since in that case the p-wave component of the pairing interaction becomes very small as it is nearly momentum independent for large values of  $\kappa^2$ . Figs. (2b),(3b) and (4b) show that for larger values of the characteristic spin-fluctuation frequency  $T_{sf}$ , the critical temperature is more sensitive to changes in  $\kappa^2$ .

Our results for the mean-field transition temperature  $T_c$  to a  $d_{x^2-y^2}$  superconducting state ( $\Phi(\mathbf{p}, i\omega_n)$  transforming as  $\cos(p_x a) - \cos(p_y a)$ ) for antiferromagnetic spin-fluctuations are shown in fig.(5). Comparing with the results displayed in fig.(3), one sees that for identical values of the characteristic spin-fluctuation temperature  $T_{sf}$ , the d-wave transition temperature saturates to a value of about  $T_{sf}/2$  for values of  $\kappa^2$  of 0.5 to 1.0, a factor of ten or

so larger than their p-wave counterparts. One also observes from figs.(3a) and (5a) that  $T_c$  saturates much more rapidly to its largest value as  $g^2$  is increased in the antiferromagnetic case than it does for ferromagnetic spin-fluctuations. One sees from figs.(3b) and (5b) that the transition temperature is much less sensitive to changes in  $\kappa^2$  in the d-wave case than it is for p-wave superconductivity. As the inverse correlation length  $\kappa^2$  is reduced, the mean-field  $T_c$  is much more robust for antiferromagnetic spin-fluctuations than for their ferromagnetic counterparts, indicating that pair-breaking effects are not as damaging in the former case. The Eliashberg renormalization factor  $Z(\mathbf{p}, i\pi T)$  is shown in figs.(6) and (7) versus wavevector  $\mathbf{p}$  for ferromagnetic and antiferromagnetic spin-fluctuations for  $\kappa^2 = 0.25$ . The average of  $Z(\mathbf{p}, i\pi T)$  over the Fermi surface as a function of  $\kappa^2$  is shown in fig.(8) for the ferromagnetic case for several values of the coupling parameter  $g^2\chi_0/t$ . We point out that even in the ferromagnetic case,  $Z$  is strongly anisotropic around the Fermi surface when the coupling parameter is small (fig.(6a)) and becomes more isotropic in the strong coupling limit (fig.(7a)). The anisotropy for small coupling parameter can be understood as a density of states effect, since the smaller Fermi velocity near the  $(\pi/a, 0)$  point can account for a larger value of  $Z$  in this region of the Brillouin Zone. These effects should matter less in the strong coupling limit. On the other hand, for antiferromagnetic spin-fluctuations, the anisotropy of  $Z$  increases as the coupling parameter is increased (see figs.(6b) and (7b)). Finally, as shown in fig.(8) for nearly ferromagnetic systems,  $Z$  increases rapidly and tends to diverge as the inverse correlation length  $\kappa \rightarrow 0$ .

#### IV. DISCUSSION

The magnetic interaction potential, Eqs. (??) is attractive everywhere for the ferromagnetic case, but oscillates in space from attractive (odd sites) to repulsive (even sites) in nearly antiferromagnetic metals. Since the average potential in the latter case tends to cancel, it may seem surprising at first sight that pairing is so much more effective in nearly antiferromagnetic than ferromagnetic metals. Part of the explanation lies in the fact that



the inner product of the spins of two interacting quasiparticles,  $\mathbf{s}_1 \cdot \mathbf{s}_2$  that enters the pairing potential, is on average three times larger in magnitude for the spin singlet than the spin triplet state for spin  $\frac{1}{2}$  particles (classically the expectation value would of course be the same in both cases). Thus the ferromagnetic interaction potential, though everywhere attractive, is for this reason alone, three times weaker than the antiferromagnetic potential. One can make this argument more quantitative and solve the Eliashberg equations for the nearly ferromagnetic metal assuming only the longitudinal spin-fluctuation mode contributes to the self-energy, setting the coupling parameter  $g^2 \rightarrow g^2/3$  in Eq. (11) (the 'Ising' case). The results of the calculations for a spin-fluctuation temperature  $T_{sf}$  equal to two thirds of the nearest neighbor hopping energy  $t$  are shown in fig.(9) and to be compared with the results shown in figs.(3) and (5). While the critical temperatures of the nearly ferromagnetic 'Ising' metal are much higher than those of the the nearly ferromagnetic one for similar conditions, they do not quite match those of the nearly antiferromagnetic case. Therefore, the factor of three in the pairing potential is not the whole story. The extra factor of  $q$  from Landau damping in Eq. (7) leads to greater incoherent scattering for a nearly ferromagnetic than antiferromagnetic metal, and hence to a reduced  $T_c$ . We have also solved the Eliashberg equations for the nearly ferromagnetic 'Ising' metal without Landau damping (with  $\eta(\hat{q}) = T_{sf}\hat{q}_+$ , in Eq. (7)). The results for the same value of  $T_{sf}$  are shown in fig.(10). One might have expected that the 'Ising' case without the Landau damping would lead to transition temperatures for the purely attractive potential and p-wave pairing that are much higher than from the spatially oscillatory potential and d-wave pairing. That this is not the case, as may be seen by comparing figs.(5) and (10), can be understood when one takes into account of the effects of retardation that restricts scattering to states within a narrow range of wavevectors near the Fermi surface. This implies that the pair wavefunction tends to oscillate in space with wavevector of the order of  $k_F$  and the probability distribution with wavevector  $2k_F$ , i.e with a wavevector comparable to that of the magnetic interaction potential itself. Furthermore, the maxima of the probability appear near the minima of the potential along the square axes, while in the d-wave state, the probability

vanishes altogether along the diagonals where the interaction is everywhere repulsive. In this case the effect of the repulsive regions is small and the gain achieved with a purely attractive potential with otherwise similar properties is not as great as might have naively been suspected.

Beside this there remains at least one more significant difference between the ferromagnetic and antiferromagnetic cases that may be relevant to pair formation but is not readily quantified. In the latter case the mass renormalization is much more anisotropic than in the former and is strongest at points on the Fermi surface (the 'hot spots') connected by the antiferromagnetic wavevector. This anisotropy may lead to strong coupling effects which on the whole are less damaging to pairing than in the corresponding ferromagnetic case where essentially all the points of the Fermi surface are equivalent.

Taken together, these effects confer a very considerable advantage for pairing to the nearly antiferromagnetic versus ferromagnetic metals that have otherwise comparable properties. Further considerations also lead to an advantage of quasi 2D over 3D metals. The average of the spin-fluctuation frequency in the Brillouin Zone tends to be larger in 2D than in 3D. This favors enhanced incoherent scattering, and hence reduced  $T_c$ . However, it also leads to an enhanced pairing energy and greater robustness against impurities and the effects of competing channels of interactions. We expect that these latter considerations will normally tend to dominate and hence favor quasi 2D over 3D systems, under otherwise similar conditions, and provided that corrections to the mean-field solutions are not important.

Within the magnetic interaction model in the mean-field approximation, thus, the highest  $T_c$  is expected to arise in quasi 2D metals with high  $T_{sf}$  and on the border of a continuous antiferromagnetic transition (when the magnetic correlation wavevector  $\kappa \rightarrow 0$  as  $T \rightarrow 0$ ). Interestingly these conditions are well satisfied in the copper oxides but much less so in the heavy fermion and organic compounds (see e.g. refs <sup>21</sup> and <sup>22</sup> respectively). In the heavy fermions  $T_{sf}$  happens to be low because the f electrons produce narrow bands, while in the organics  $T_{sf}$  is small because the carrier concentration is low. Thus one expects, and indeed one finds, much lower  $T_c$ 's in these materials than in the cuprates.

The calculations also predict that magnetically mediated superconductivity should be a general phenomenon occurring on the boundary of a continuous magnetic transition, in both ferromagnets and antiferromagnets and in quasi 2D and 3D compounds. This may not be observed in practice, however, due to pair breaking effects of impurities and other interaction channels not considered here explicitly. In cases when the magnetic transition is not abrupt and  $\kappa$  can be made arbitrarily small at low temperatures, the magnetic interaction potential may overwhelm these other effects and, at least in the nearly antiferromagnetic case where the mean-field  $T_c$  appears to remain finite as  $\kappa \rightarrow 0$ , superconductivity may survive in a narrow range of lattice densities near the critical density where the magnetic order is continuously quenched.

The magnetic interaction model and the mean-field approximation for  $T_c$  might be expected to apply most successfully in nearly magnetic metals where  $T_c$  is small compared to the electronic bandwidth and  $T_{sf}$ . The nearly ferromagnetic quasi 2D metal  $Sr_2RuO_4$  that orders in a spin-triplet p-wave state only at very low temperatures (below  $1.5^\circ K$ ),<sup>25,17,29,24,12-16</sup> would therefore seem an ideal candidate for comparison between theory and experiment. The calculations presented in this paper provide a first step toward such a comparison. The next will be to build a realistic model of  $\chi(\mathbf{q}, \omega)$  from NMR and neutron scattering measurements, or from the numerical calculations now in progress<sup>18</sup>. Preliminary evidence suggests that  $Sr_2RuO_4$  may be close both to ferromagnetism and antiferromagnetism<sup>28</sup>. The competition between these two tendencies, along with the comparatively small magnitude of  $\langle \mathbf{s}_1 \cdot \mathbf{s}_2 \rangle$  in the observed spin-triplet state and other features as discussed above, may help to account for the much lower  $T_c$  in this layer perovskite oxide compared with that of the cuprates.

We note that our calculations may be expected to break down when the mass renormalization becomes large at high values of the coupling constant or at small  $\kappa$  near the critical point for magnetic order. Also it should fail when the superconducting coherence length becomes small compared with the average spacing between Cooper pairs, i.e. for sufficiently high  $T_c$  or in *strictly* 2D where there is no true long-range order at finite temperature. The

latter condition is not readily reached in many of the known quasi 2D systems.

Finally, we emphasize that our model for the magnetic interaction does not include any possible spin-gap formation. For this reason alone, it is not expected to apply near the metal-insulator phase boundary in the cuprates<sup>23</sup>.

## V. CONCLUSIONS

We have contrasted the predictions for the superconducting transition temperature for magnetically mediated superconductivity for nearly ferromagnetic versus nearly antiferromagnetic metals in quasi 2D. The calculations are based on a single Fermi surface sheet, and a conventional form for the magnetic interaction arising from the exchange of spin fluctuations treated in the mean-field Eliashberg theory. The dominant  $\mathbf{q}$  and  $\omega$  dependence of this interaction is assumed to arise from the dynamical wavevector dependence of the susceptibility, and thus the interaction vertex is taken to be a phenomenological constant. In principle the latter quantities may be inferred independently from inelastic neutron scattering and for example the temperature dependence of the resistivity in the normal state. The mean-field Eliashberg theory is expected to break down when, for example,  $T_c$  is so high that the superconducting coherence length becomes small and less than the typical spatial separation of Cooper pairs. It may also fail in the immediate vicinity of the critical density when magnetic order is quenched continuously and the quasiparticle density of states tends to become singular. Here the electron quasiparticle framework underpinning the mean-field Eliashberg model may break down in an essential and non-trivial fashion.

Within the range of validity of our calculations we may conclude that, for the same set of dimensionless parameters, the p-wave triplet pairing in nearly ferromagnetic metals is much less robust than the d-wave singlet pairing in the corresponding nearly antiferromagnetic metals. For values of  $T_{sf}$  that are typical of d metals in the layered perovskites, we predict a maximum of  $T_c$  versus  $\kappa$  of the order of  $100^\circ K$  in the latter but typically one or more orders of magnitude less than this in the former. The reasons for the dramatic difference

are discussed in section IV.

The pair breaking effects of impurities and of competing interaction channels can lead to substantially lower values than the above in real materials. These effects may, however, be mitigated by reducing  $\kappa$  via some external control parameter such as pressure and hence enhancing the magnetic pairing energy.

The calculations are intriguing in the light of the d-wave singlet state observed in the cuprates with strongly enhanced antiferromagnetic susceptibilities and  $T_c$ 's of the order of  $100^\circ K$ , versus the p-wave triplet state found in the ruthenate  $Sr_2RuO_4$  that is close to ferromagnetic order and has a much lower  $T_c$  (of the order of  $1^\circ K$ ).

The maximum of  $T_c$  versus  $\kappa$  in  $Sr_2RuO_4$  in the triplet state is not yet known, and may well be higher than that measured at ambient pressure. A more complete description of  $Sr_2RuO_4$  must await realistic modelling of the dynamical susceptibility which may reflect not only ferromagnetic but also competing antiferromagnetic tendencies. The latter may be subdominant at ambient pressure but may be highly sensitive to lattice spacing. It would also be interesting to investigate more closely the effect of the additional Fermi surface sheets in  $Sr_2RuO_4$ . An experimental study of the variation of  $T_c$  vs  $\kappa$  in this system, that satisfies to a greater extent than cuprates the condition  $T_c \ll T_{sf}$ , would provide a vital test of the theory of magnetically mediated superconductivity. Such a study would be feasible in  $Sr_2RuO_4$  if it orders ferromagnetically at positive pressure<sup>16</sup>, and in the isostructural and isoelectronic compounds  $Ca_2RuO_4$  and  $Sr_2FeO_4$  that are expected to become similar to  $Sr_2RuO_4$  at very high pressure.

Finally we reiterate that our calculations suggests that one should look for elevated transition temperatures in systems in which (i)  $T_{sf}$  is high, i.e. the electron density is not too low and effective band mass not too high, (ii) the lattice or carrier density can be tuned to the vicinity of a magnetic critical point in the metallic state, (iii) the electronic structure is quasi 2D rather than 3D, and (iv) antiferromagnetism (or 'Ising' ferromagnetism) is favored over ferromagnetism. A considerable number of candidate materials for further study of the predictions of the magnetic pairing model would seem to be available given current

material fabrication and high pressure technology. The experimental investigation of such systems, whether or not they prove to yield high transition temperatures, should help us to improve our understanding of magnetic pairing and perhaps also shed light on the more exotic models<sup>23</sup> for normal and superconducting states that have been proposed for highly correlated electronic systems.

## **VI. ACKNOWLEDGMENTS**

We would like to thank P. Coleman, S.R. Julian, P.B. Littlewood, A.J. Millis, A.P. Mackenzie, D. Pines, D.J. Scalapino and M. Sigrist for discussions on this and related topics. We acknowledge the support of the EPSRC and the Royal Society.

## REFERENCES

- <sup>1</sup> W. Hardy et al., Phys. Rev. Lett. **70**, 399 (1993).
- <sup>2</sup> D. Wollman et al., Phys. Rev. Lett. **71**, 2134 (1993).
- <sup>3</sup> D.J. Van Harlingen, Rev. Mod. Phys. **67**, 515 (1995).
- <sup>4</sup> J. Kirtley et al., Nature **373**, 225 (1995).
- <sup>5</sup> J. Kirtley et al., Phys. Rev. Lett **76**, 1336 (1996).
- <sup>6</sup> K. Miyake, S. Schmitt-Rink and C.M. Varma, Phys. Rev. B **34**, 6654 (1986).
- <sup>7</sup> N.E. Bickers, D.J. Scalapino and R.T. Scalettar, Inter. J. Mod. Phys B **1**, 687 (1987).
- <sup>8</sup> N.E. Bickers, D.J. Scalapino and S.R. White, Phys. Rev. Lett. **62**, 961 (1989).
- <sup>9</sup> T. Moriya , Y. Takahashi and K. Ueda, J. Phys. Soc. Jpn. **59**, 2905 (1990).
- <sup>10</sup> P. Monthoux and D. Pines, Phys. Rev. Lett. **69**, 961 (1992) and Phys. Rev. B **47**, 6069 (1993).
- <sup>11</sup> C.-H. Pao and N.E. Bickers, Phys. Rev. B **49**, 1586 (1994).
- <sup>12</sup> G.M. Luke et al., Nature **394**, 558 (1998).
- <sup>13</sup> T.M. Riseman et al., Nature **396**, 242 (1998).
- <sup>14</sup> K. Ishida et al., Nature **396**, 658 (1998).
- <sup>15</sup> A.P. Mackenzie et al., Phys. Rev. Lett. **80**, 161 (1998).
- <sup>16</sup> K. Yoshida et al., Phys. Rev. B **58**, 15062 (1998).
- <sup>17</sup> T.M. Rice and M. Sigrist, J. Phys. C **7**, L643 (1997).
- <sup>18</sup> I.I. Mazin and D.J. Singh, Phys. Rev. Lett. **79**, 733 (1997).
- <sup>19</sup> K. Levin and O.T. Valls, Phys. Rev. B **17**, 191 (1978).

- <sup>20</sup> D. Fay and J. Appel, Phys. Rev. B **22**, 3173 (1980).
- <sup>21</sup> D. Jerome, Organic Conductors (Dekker, New York, 1994).
- <sup>22</sup> N. Mathur et al., Nature **394**, 39 (1998).
- <sup>23</sup> P.W. Anderson, Theory of Superconductivity of High- $T_c$  Cuprate Superconductors (Princeton Univ. Press, 1997).
- <sup>24</sup> Y. Maeno et al., Nature **372**, 532 (1994).
- <sup>25</sup> D.F. Agterberg, T.M. Rice and M. Sigrist, Phys. Rev. Lett. **78**, 3374 (1997).
- <sup>26</sup> S. Nakamura, T. Moriya and K. Ueda, J. Phys. Soc. Jpn. **65**, 4026 (1996).
- <sup>27</sup> P. Monthoux and D. Pines, Phys. Rev. B **49**, 4261 (1994).
- <sup>28</sup> I.I. Mazin and D.J. Singh, preprint cond-mat/9902193.
- <sup>29</sup> G. Baskaran, Physica **223B-224B**, 490 (1996).



## FIGURES

FIG. 1. The Fermi surface for  $t' = 0.45t$  and electron density  $n = 1.1$ .

FIG. 2. The mean-field critical temperature  $T_c$  to the p-wave superconducting state versus  $g^2\chi_0/t$  for  $\kappa^2 = 0.25, 0.50, 1.0, 2.0, 3.0, 4.0$  (a) and versus  $\kappa^2$  for  $g^2\chi_0/t = 60, 30, 20, 10, 5$  (b). The characteristic spin-fluctuation temperature is  $T_{sf} = 0.33t$  with  $\kappa_0^2 = 24$ .

FIG. 3. The mean-field critical temperature  $T_c$  to the p-wave superconducting state versus  $g^2\chi_0/t$  for  $\kappa^2 = 0.25, 0.50, 1.0, 2.0, 3.0, 4.0$  (a) and versus  $\kappa^2$  for  $g^2\chi_0/t = 60, 30, 20, 10, 5$  (b). The characteristic spin-fluctuation temperature is  $T_{sf} = 0.67t$  with  $\kappa_0^2 = 12$ .

FIG. 4. The mean-field critical temperature  $T_c$  to the p-wave superconducting state versus  $g^2\chi_0/t$  for  $\kappa^2 = 0.25, 0.50, 1.0, 2.0, 3.0, 4.0$  (a) and versus  $\kappa^2$  for  $g^2\chi_0/t = 60, 30, 20, 10, 5$  (b). The characteristic spin-fluctuation temperature is  $T_{sf} = 1.33t$  with  $\kappa_0^2 = 6$ .

FIG. 5. The mean-field critical temperature  $T_c$  to the d-wave superconducting state versus  $g^2\chi_0/t$  for  $\kappa^2 = 0.25, 0.50, 1.0, 2.0, 3.0, 4.0$  (a) and versus  $\kappa^2$  for  $g^2\chi_0/t = 60, 30, 20, 10, 5$  (b). The characteristic spin-fluctuation temperature is  $T_{sf} = 0.67t$  with  $\kappa_0^2 = 12$ .

FIG. 6. The Eliashberg renormalization factor  $Z(\mathbf{p}, i\pi T) = 1 - \text{Im}\Sigma(\mathbf{p}, i\pi T)/\pi T$  versus wavevector  $\mathbf{p}$  for ferromagnetic (a) and antiferromagnetic spin-fluctuations (b) for  $g^2\chi_0/t = 5$ ,  $\kappa^2 = 0.25$  and  $T = 0.00625t$ . The characteristic spin-fluctuation temperature is  $T_{sf} = 0.67t$  and  $\kappa_0^2 = 12$ .

FIG. 7. The Eliashberg renormalization factor  $Z(\mathbf{p}, i\pi T) = 1 - \text{Im}\Sigma(\mathbf{p}, i\pi T)/\pi T$  versus wavevector  $\mathbf{p}$  for ferromagnetic (a) and antiferromagnetic spin-fluctuations (b) for  $g^2\chi_0/t = 30$ ,  $\kappa^2 = 0.25$  and  $T = 0.00625t$ . The characteristic spin-fluctuation temperature is  $T_{sf} = 0.67t$  and  $\kappa_0^2 = 12$ .

FIG. 8. The Eliashberg renormalization factor  $Z(\mathbf{p}, i\pi T) = 1 - \text{Im}\Sigma(\mathbf{p}, i\pi T)/\pi T$  averaged over the Fermi surface for ferromagnetic spin-fluctuations versus  $\kappa^2 = 0.25$  for  $g^2\chi_0/t = 5, 10$  and  $30$ , and  $T = 0.003125t$ . The characteristic spin-fluctuation temperature is  $T_{sf} = 0.67t$  and  $\kappa_0^2 = 12$ .

FIG. 9. The mean-field critical temperature  $T_c$  to the p-wave 'Ising' superconducting state versus  $g^2\chi_0/t$  for  $\kappa^2 = 0.25, 0.50, 1.0, 2.0, 3.0, 4.0$  (a) and versus  $\kappa^2$  for  $g^2\chi_0/t = 60, 30, 20, 10, 5$  (b). The characteristic spin-fluctuation temperature is  $T_{sf} = 0.67t$  with  $\kappa_0^2 = 12$ . For the same value of the coupling parameter the effective mass for 'Ising' p-wave pairing is much lower than for the standard p-wave state. That explains the more rapid drop of  $T_c$  as  $\kappa \rightarrow 0$  in fig.(3) than in the above figure.

FIG. 10. The mean-field critical temperature  $T_c$  to the p-wave 'Ising' superconducting state without Landau damping versus  $g^2\chi_0/t$  for  $\kappa^2 = 0.25, 0.50, 1.0, 2.0, 3.0, 4.0$  (a) and versus  $\kappa^2$  for  $g^2\chi_0/t = 60, 30, 20, 10, 5$  (b). The characteristic spin-fluctuation temperature is  $T_{sf} = 0.67t$  with  $\kappa_0^2 = 12$ .

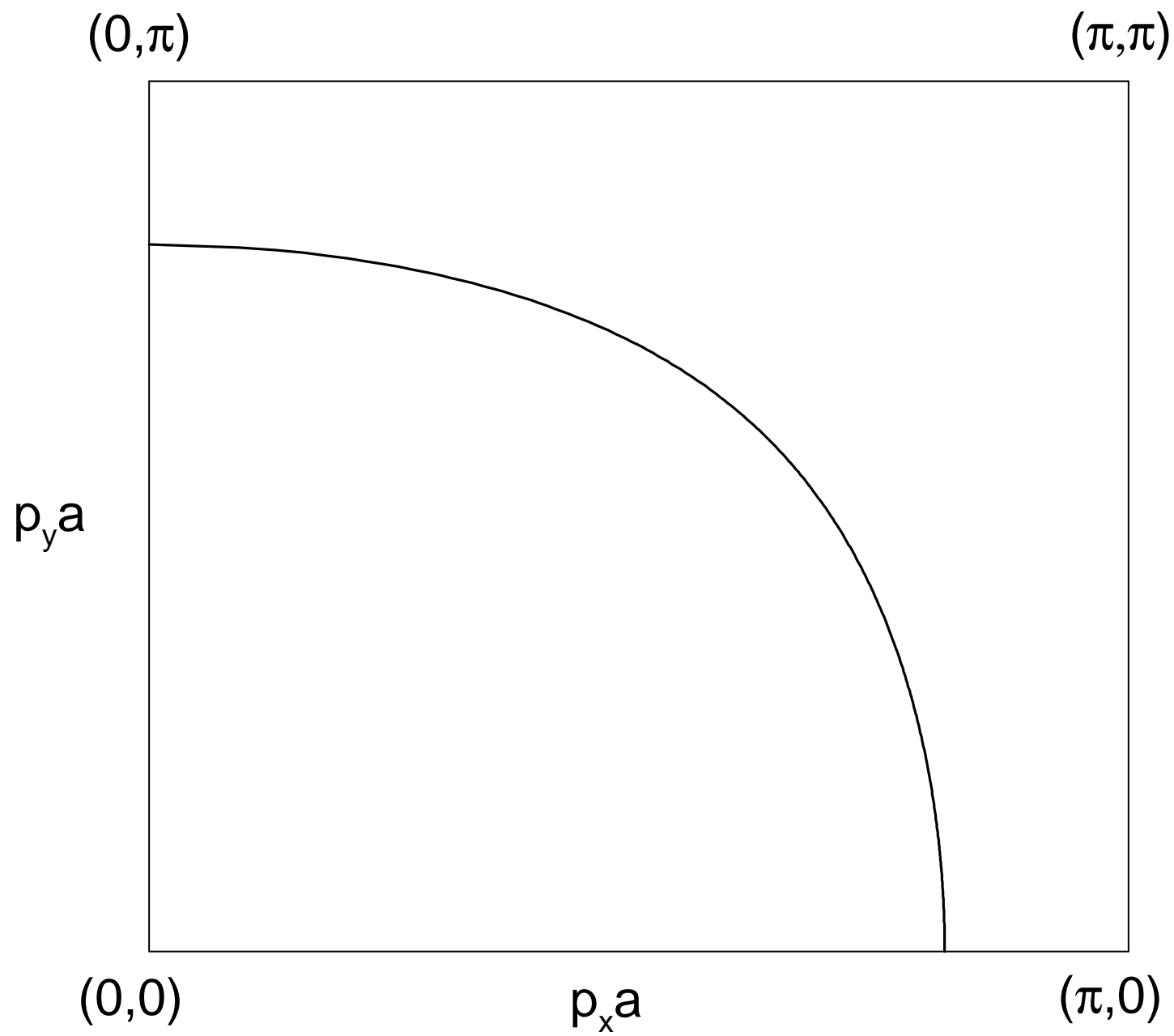


fig.1

$$T_{\text{sf}} = 0.33t ; \kappa_0^2 = 24$$

p-wave

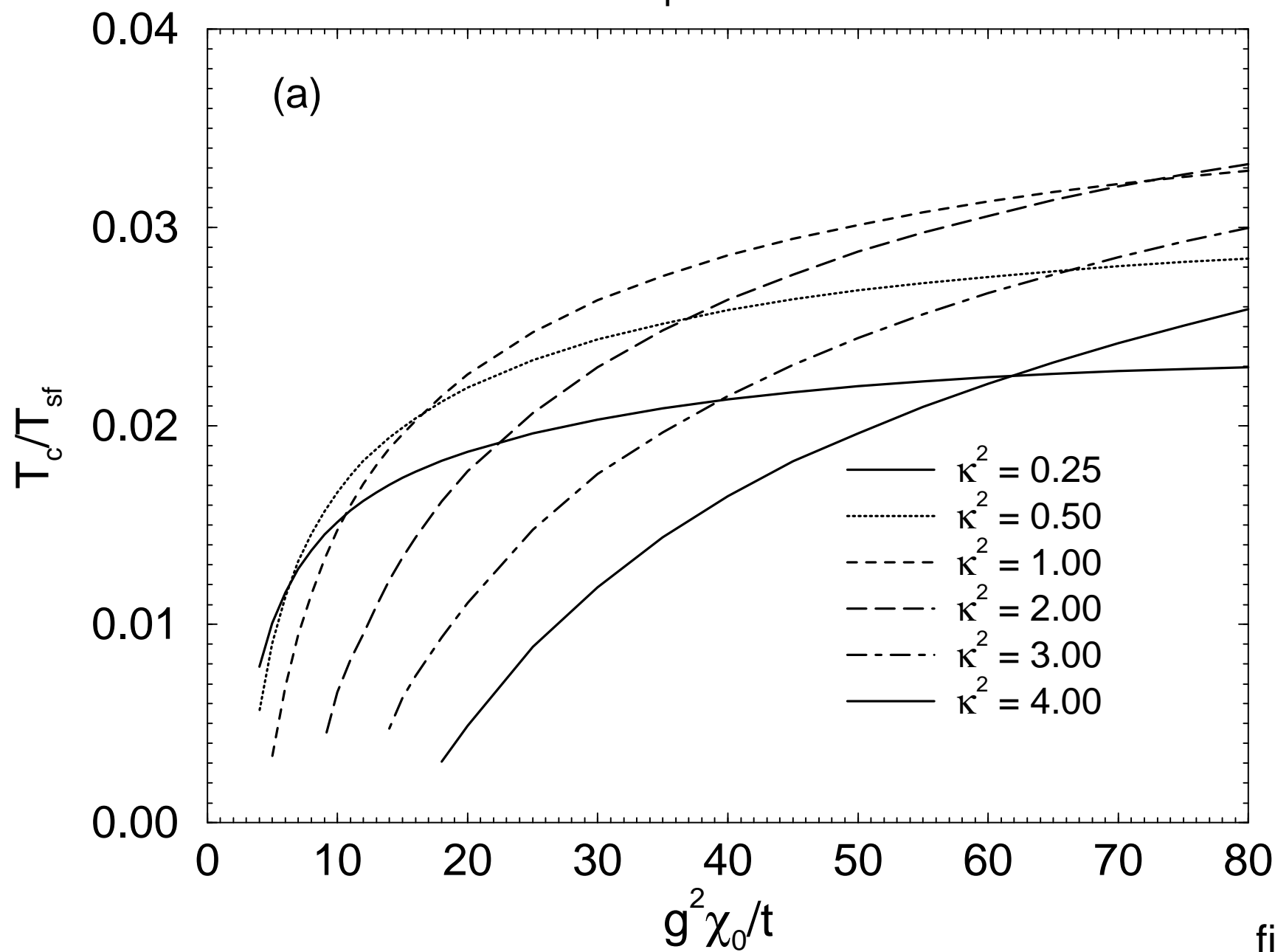


fig.2

$$T_{\text{sf}} = 0.33t ; \kappa_0^2 = 24$$

p-wave

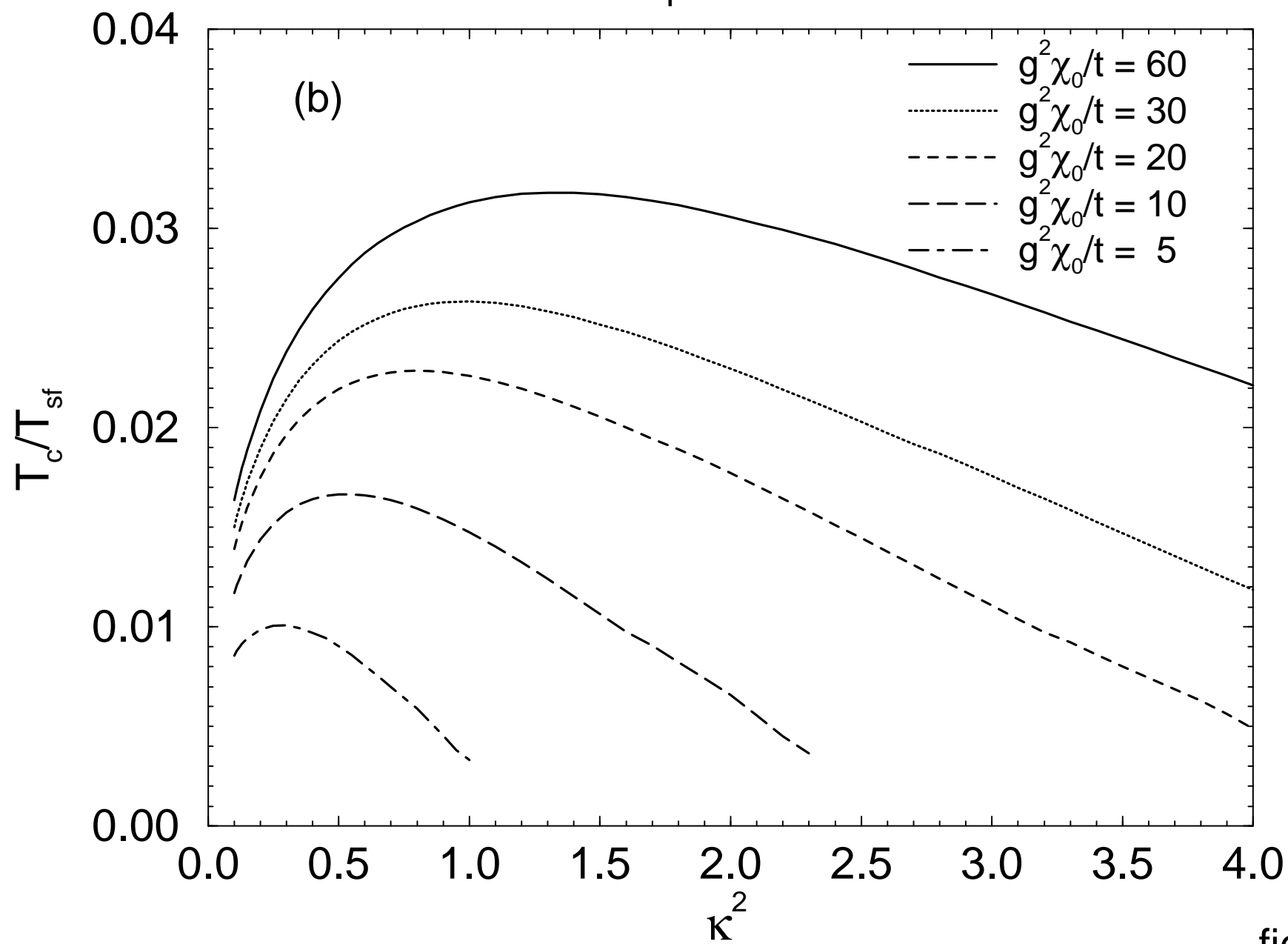


fig.2

$$T_{\text{sf}} = 0.67t ; \kappa_0^2 = 12$$

p-wave

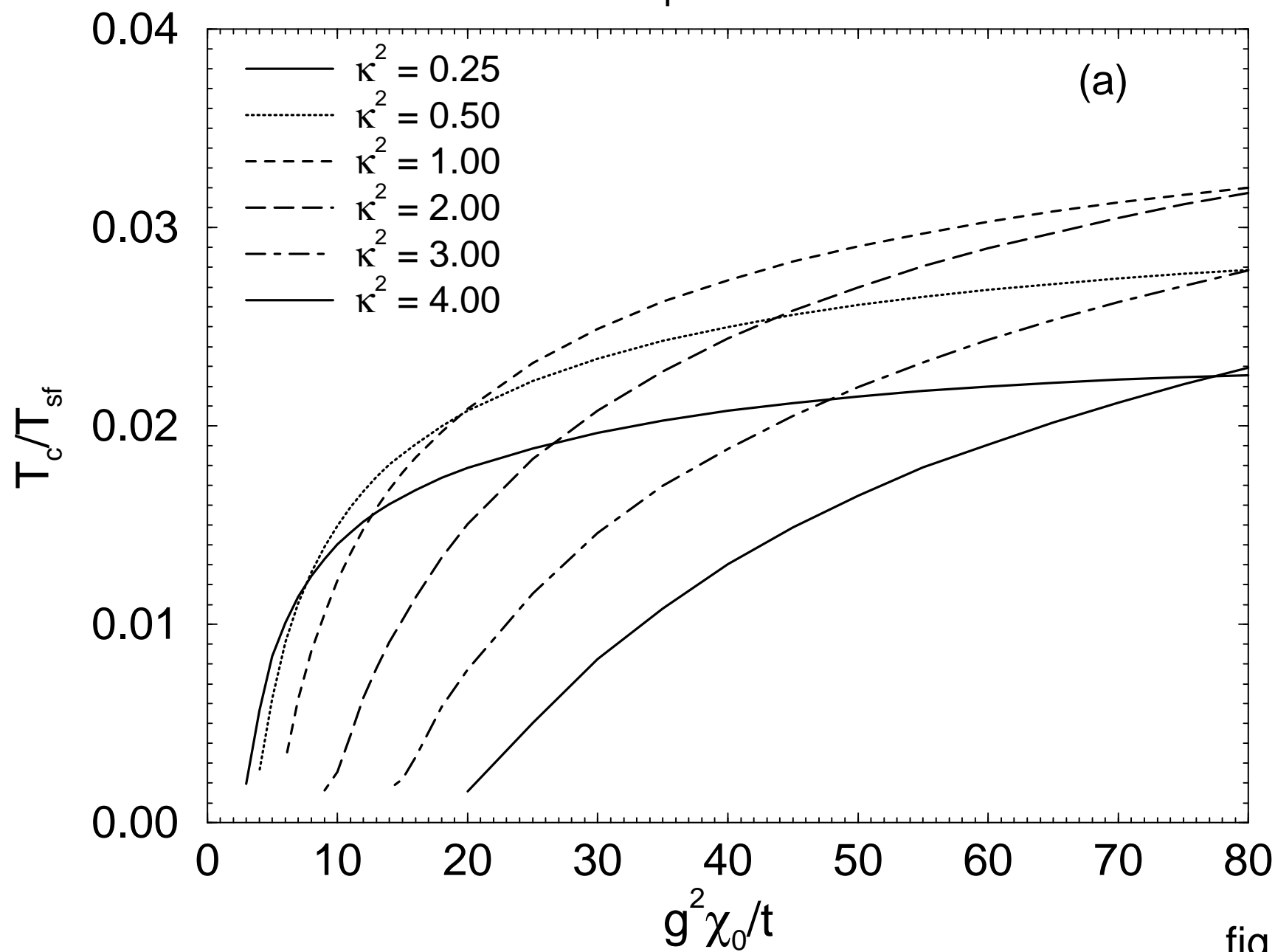


fig.3

$$T_{\text{sf}} = 0.67t ; \kappa_0^2 = 12$$

p-wave

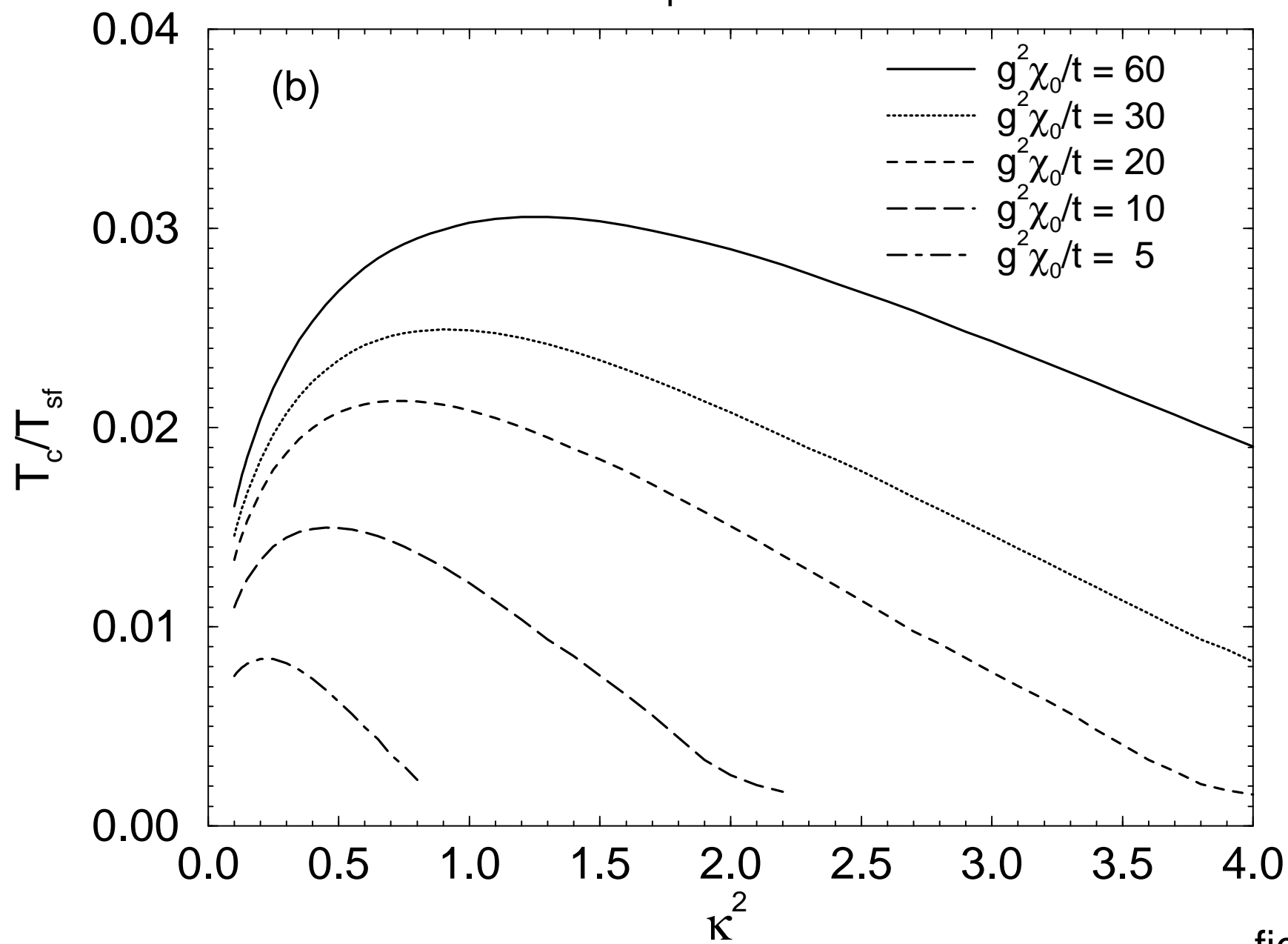


fig.3

$$T_{\text{sf}} = 1.33t ; \kappa_0^2 = 6$$

p-wave

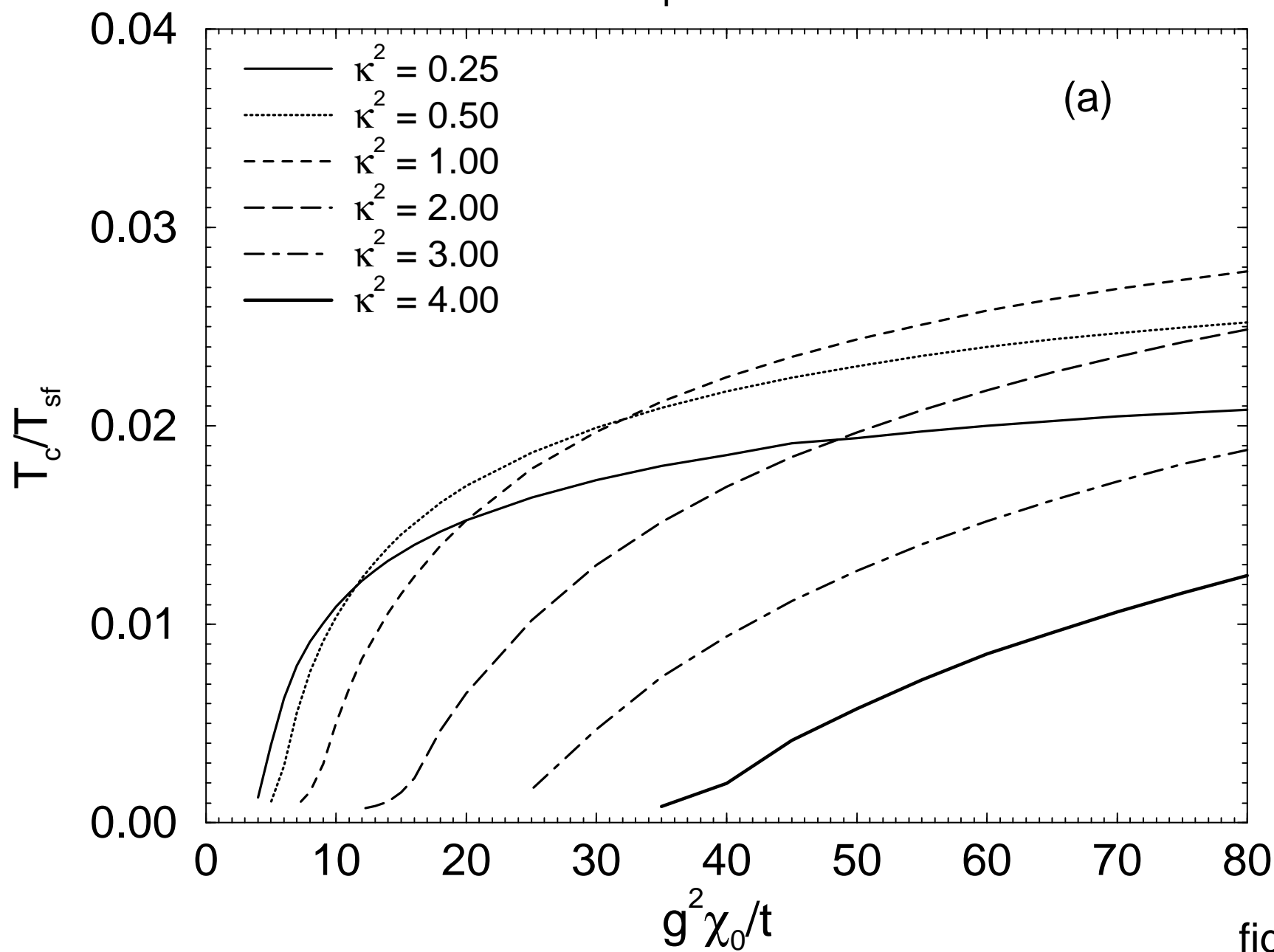


fig.4



$$T_{\text{sf}} = 1.33t ; \kappa_0^2 = 6$$

p-wave

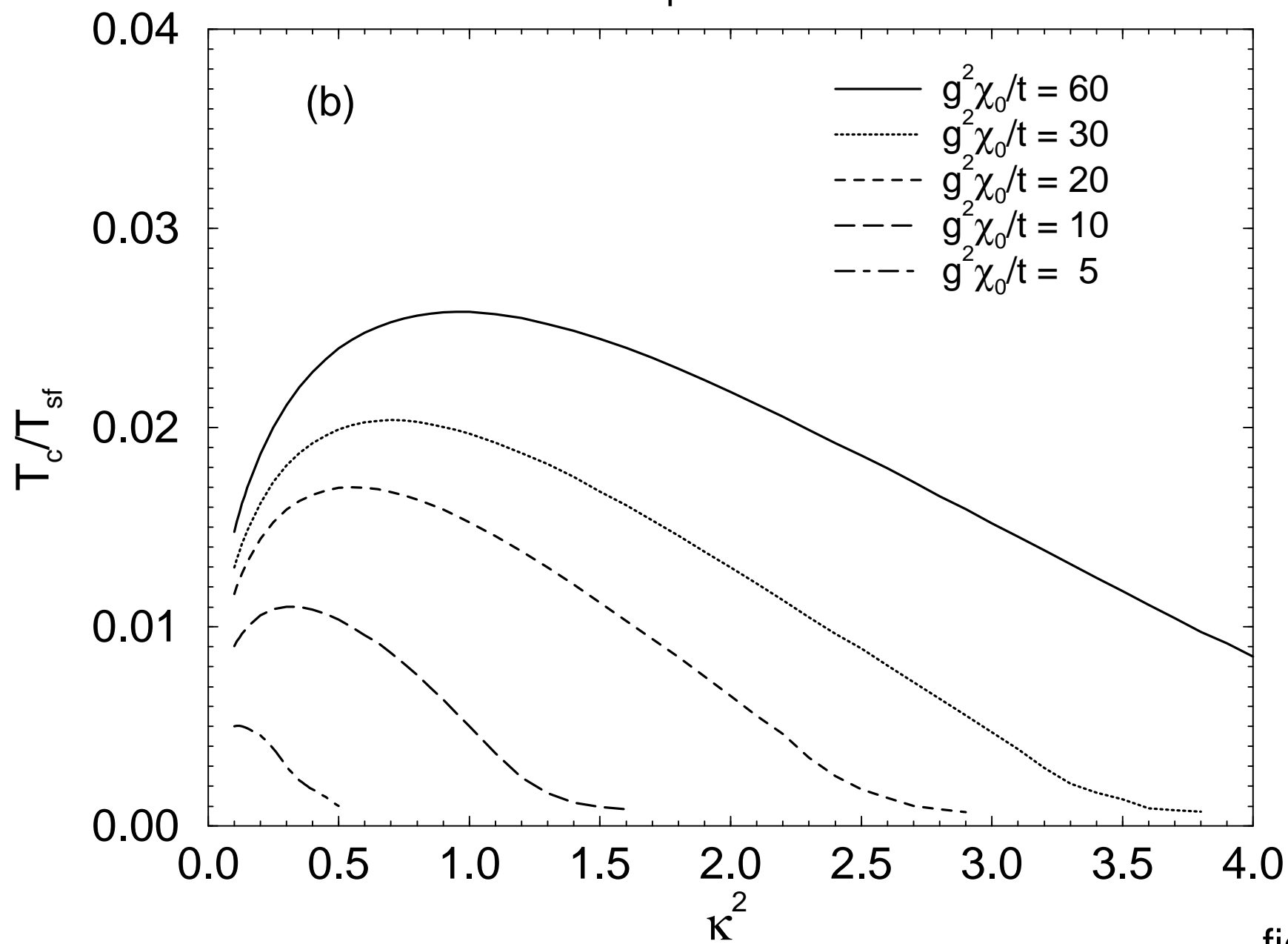


fig.4

$$T_{\text{sf}} = 0.67t; \kappa_0^2 = 12$$

d-wave

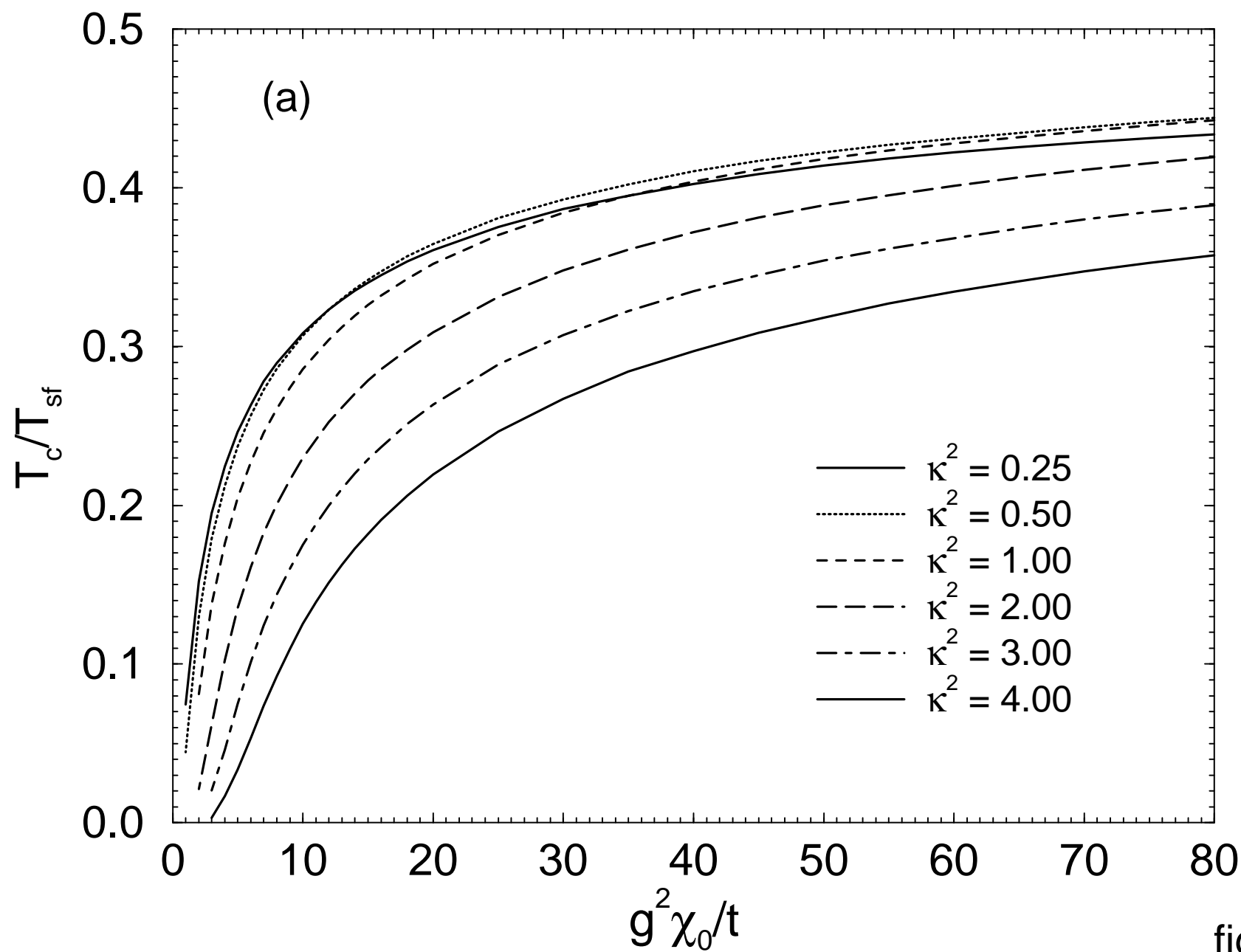


fig.5

$$T_{\text{sf}} = 0.67t ; \kappa_0^2 = 12$$

d-wave

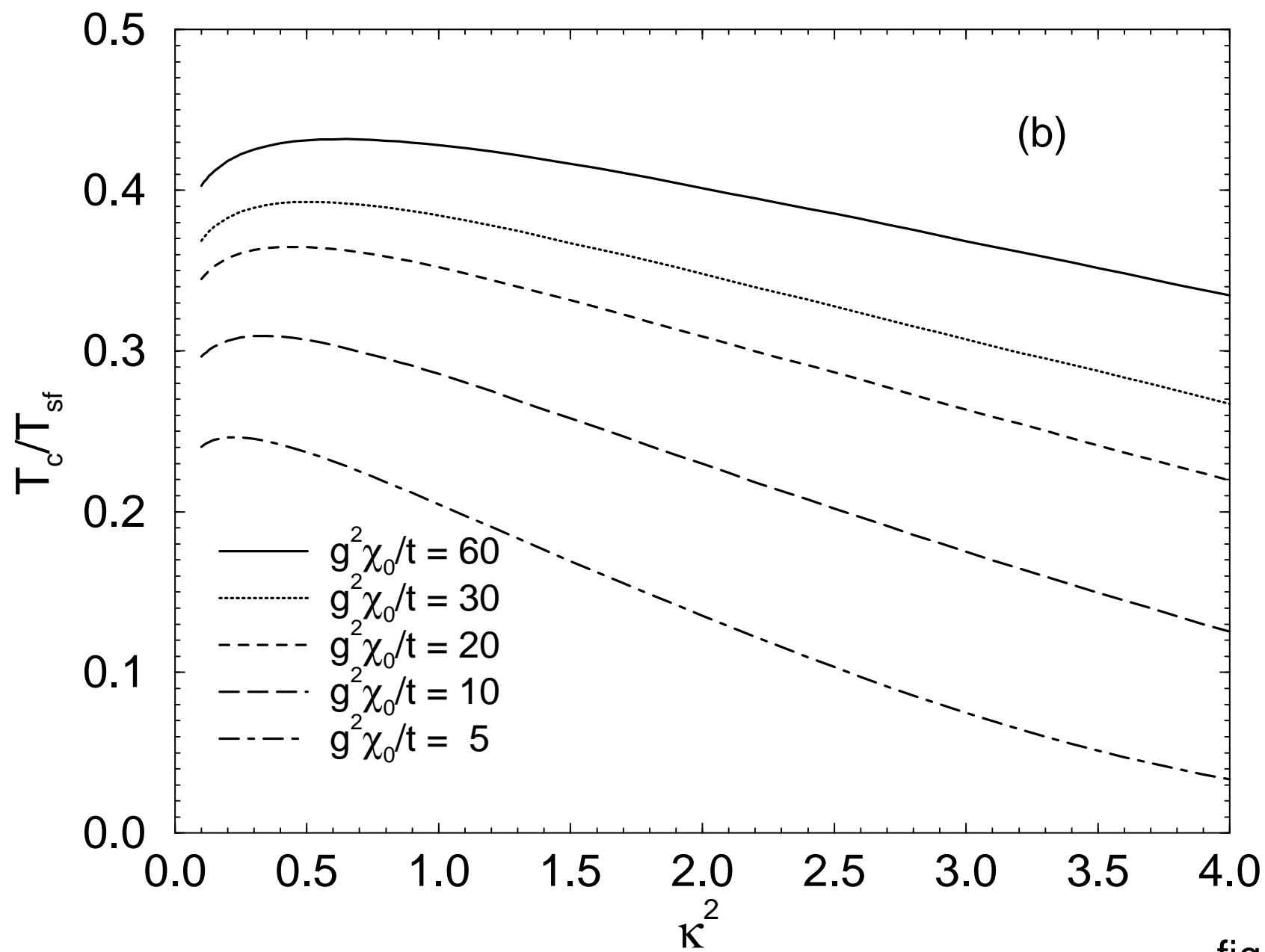


fig.5

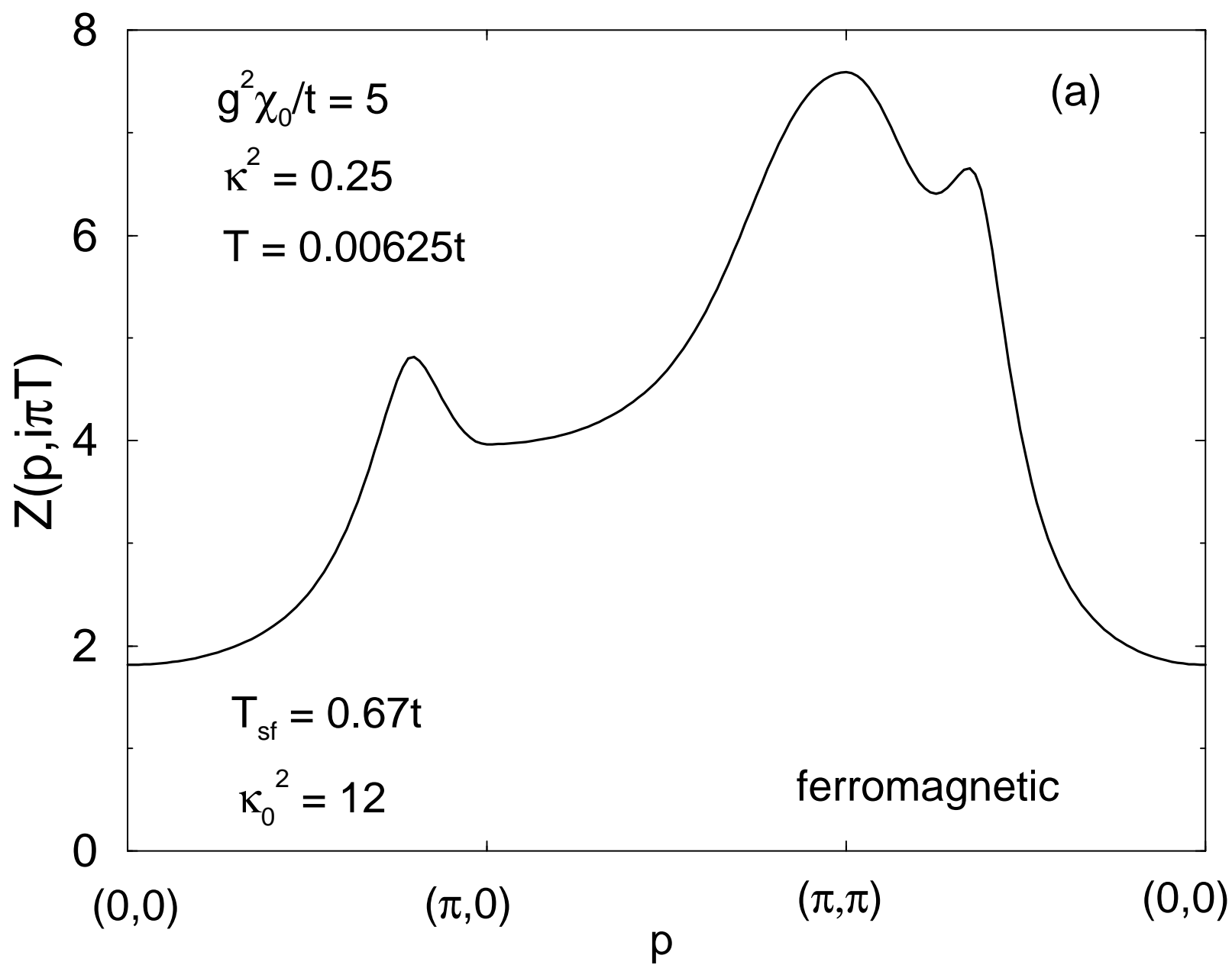


fig. 6

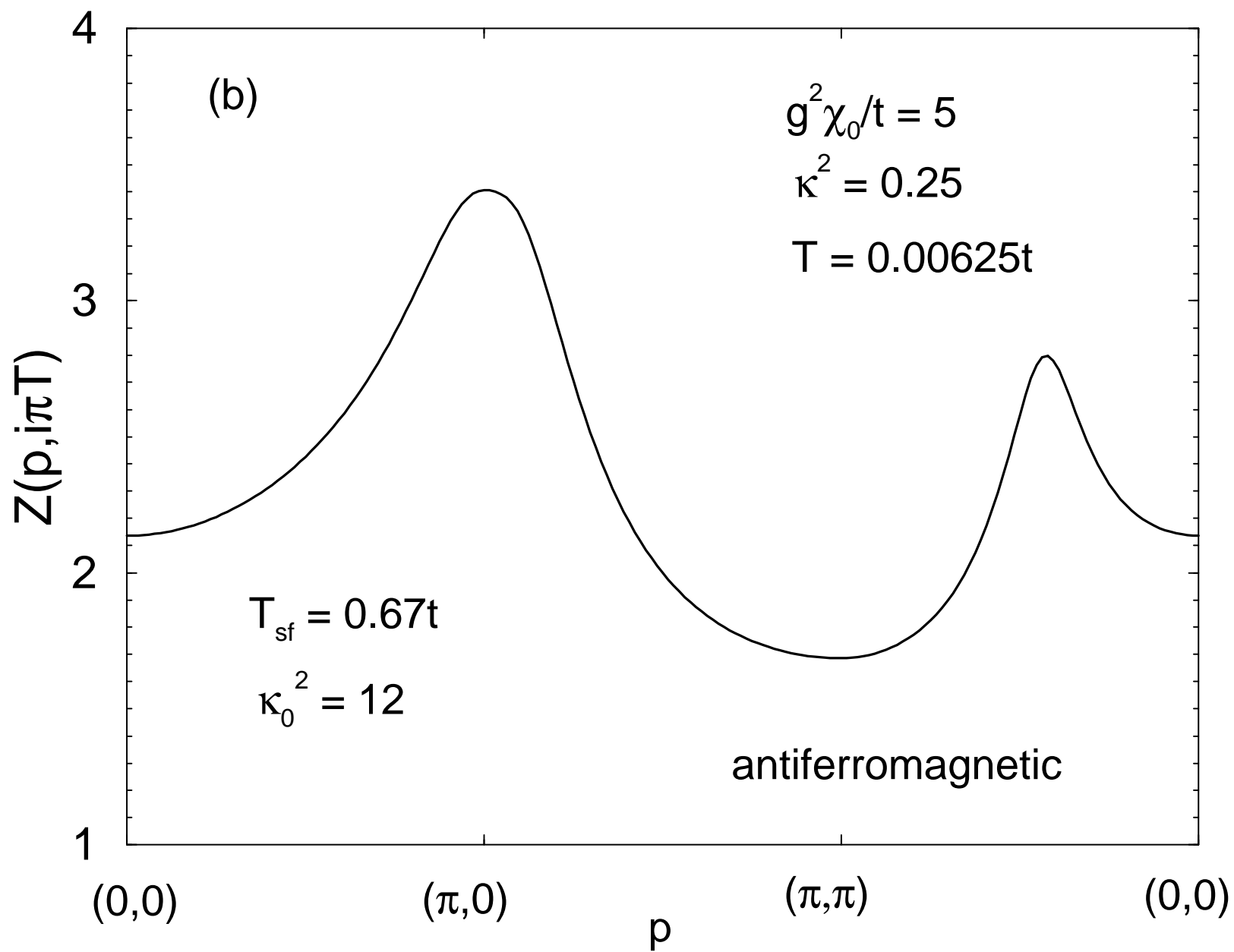


fig.6

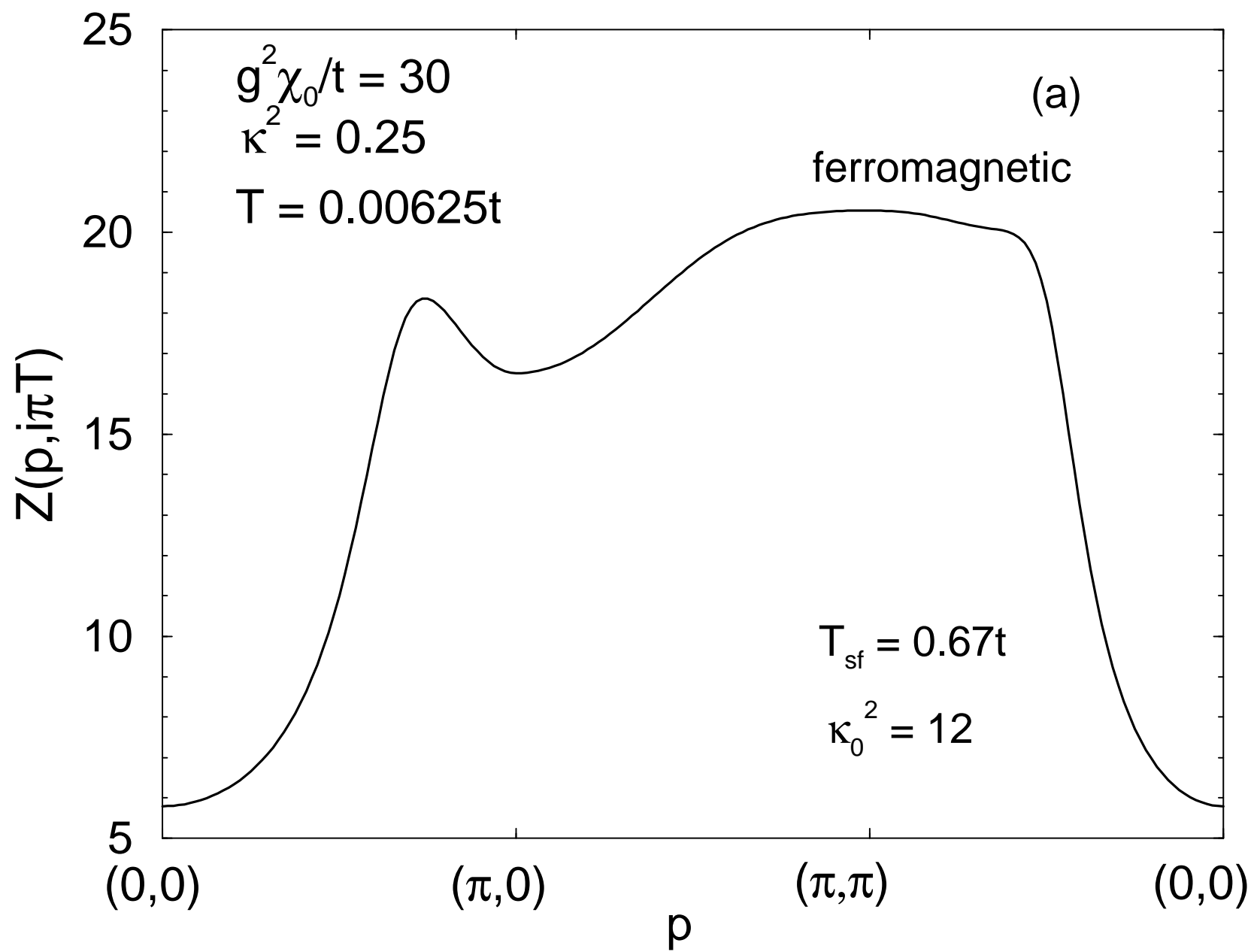


fig.7

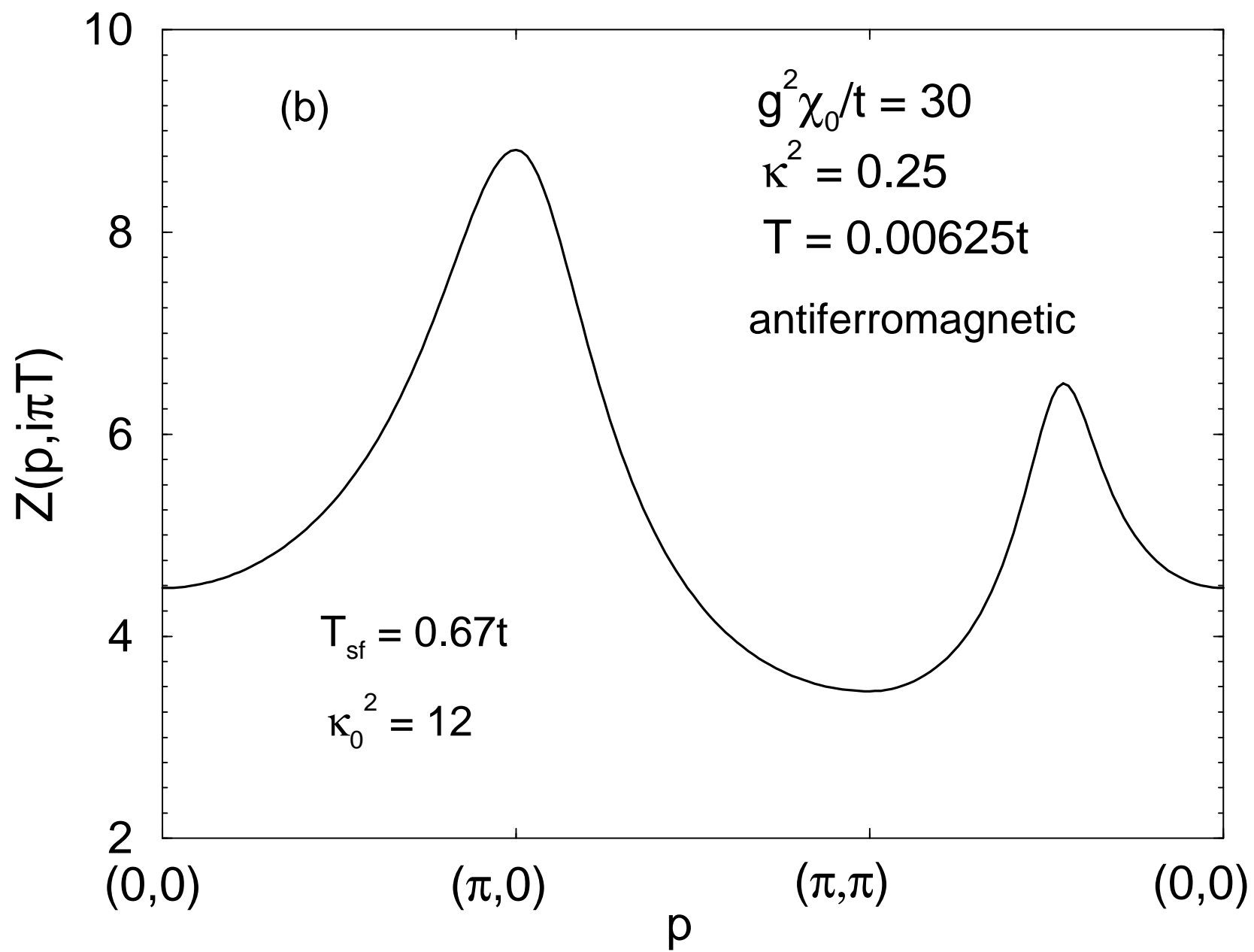


fig.7

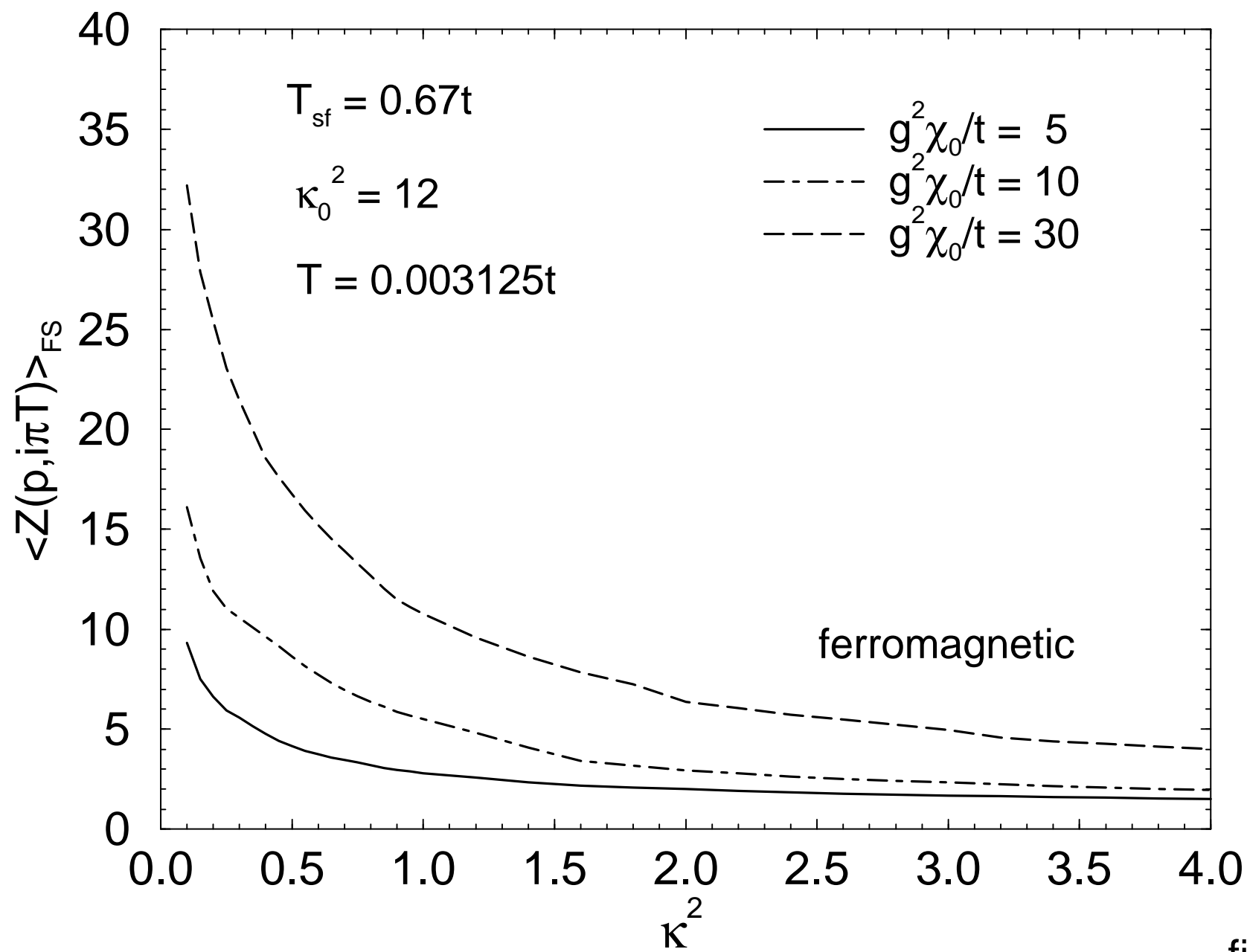


fig. 8



$T_{\text{sf}} = 0.67t ; \kappa_0^2 = 12$   
'Ising' p-wave

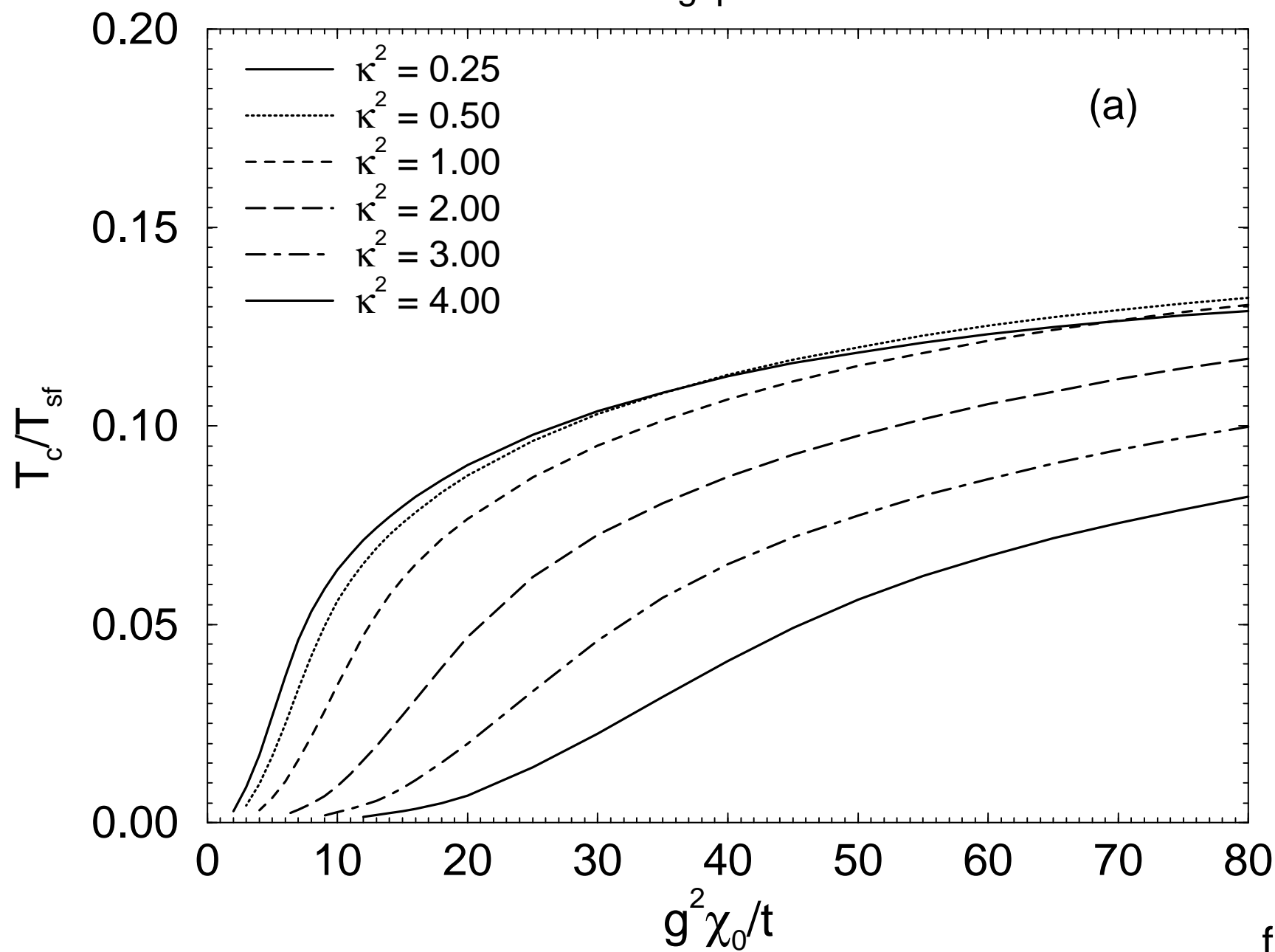


fig.9

$T_{\text{sf}} = 0.67t ; \kappa_0^2 = 12$   
'Ising' p-wave

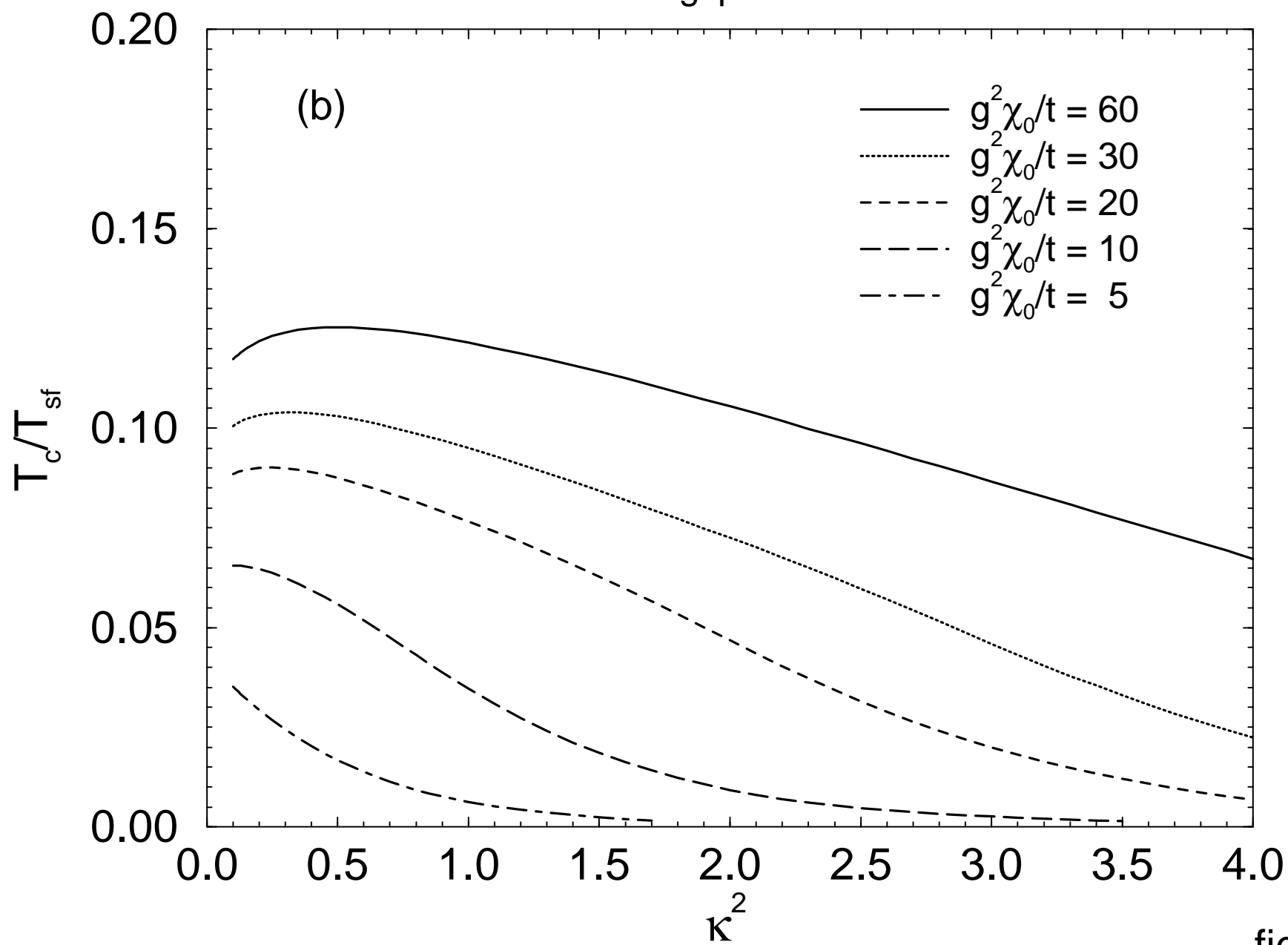


fig.9

$T_{\text{sf}} = 0.67t$  ;  $\kappa_0^2 = 12$   
 'Ising' p-wave, no Landau damping

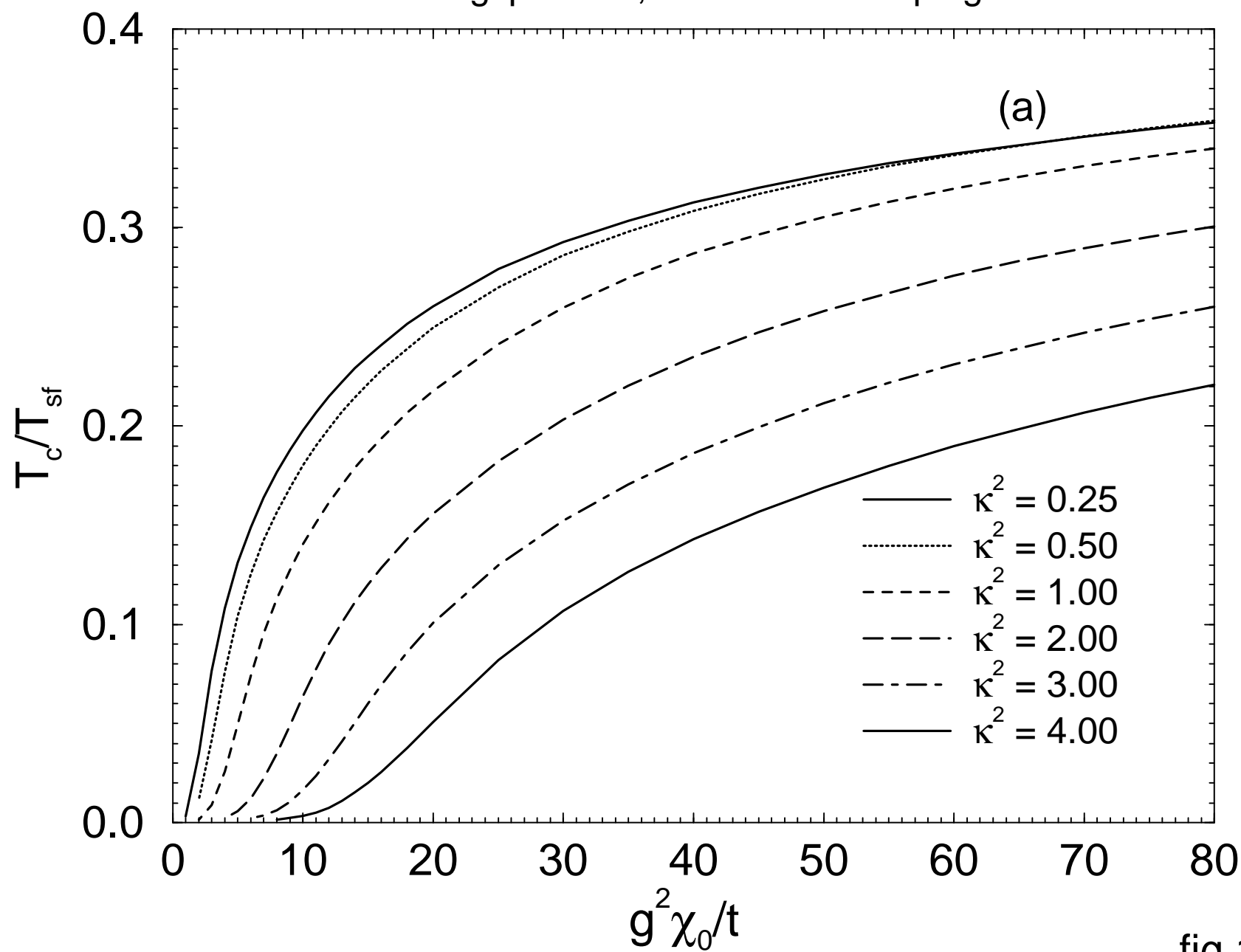


fig.10

$T_{\text{sf}} = 0.67t ; \kappa_0^2 = 12$   
 'Ising' p-wave, no Landau damping

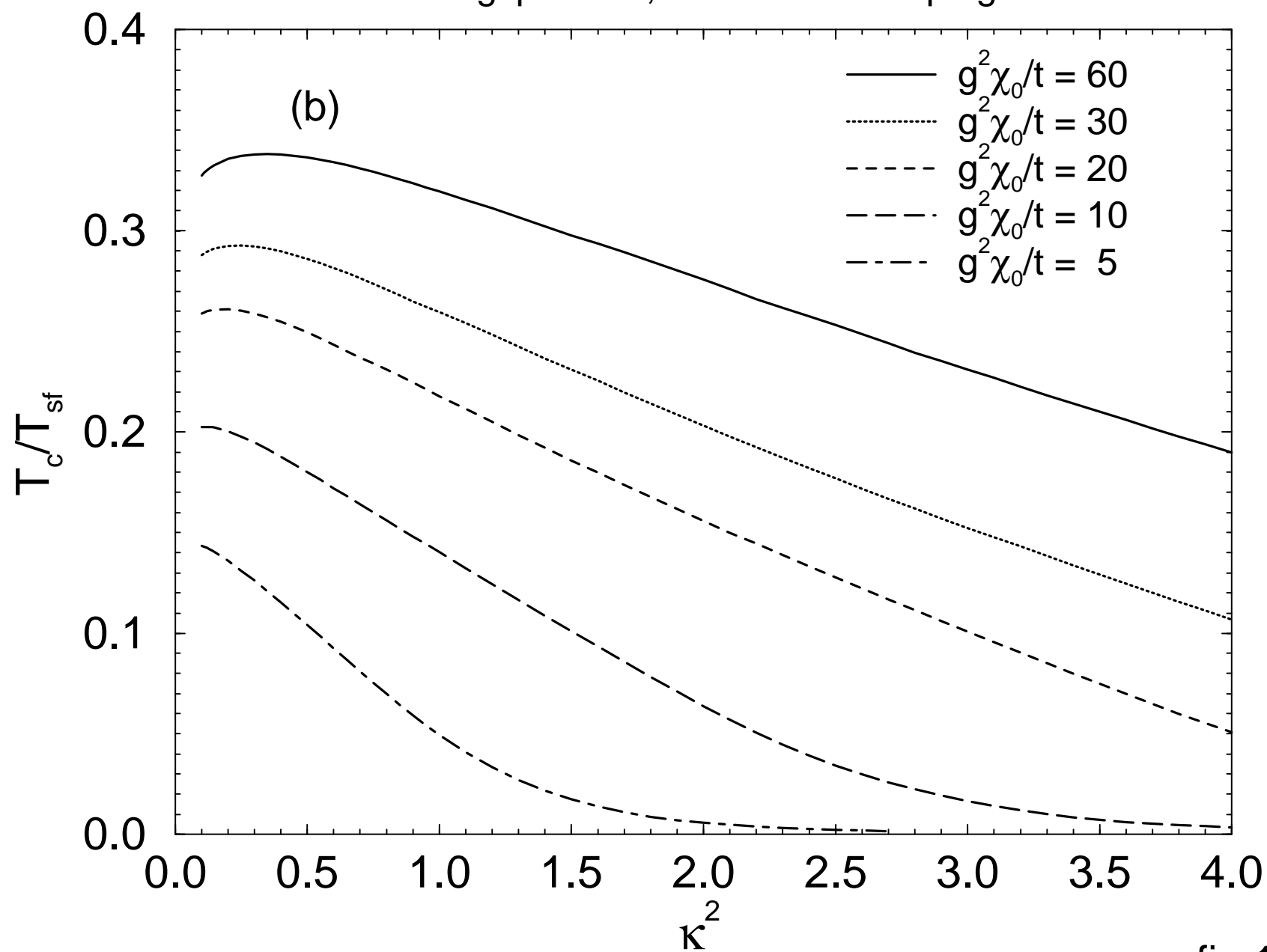


fig.10